coatings

MDPI

Article

Influence of Material Composition on Structural and Optical Properties of HfO_2-TiO_2 Mixed Oxide Coatings

Michal Mazur *, Danuta Kaczmarek, Jaroslaw Domaradzki, Damian Wojcieszak and Agata Poniedzialek

Wroclaw University of Technology, Faculty of Microsystem Electronics and Photonics, Janiszewskiego 11/17, 50-372 Wroclaw, Poland; danuta.kaczmarek@pwr.edu.pl (D.K.); jaroslaw.domaradzki@pwr.edu.pl (J.D.); damian.wojcieszak@pwr.edu.pl (D.W.); agata.poniedzialek@pwr.edu.pl (A.P.)

* Correspondence: michal.mazur@pwr.edu.pl; Tel.: +48-71-320-33-22; Fax: +48-71-328-35-04

Academic Editor: Desmond Gibson

Received: 18 January 2016; Accepted: 17 March 2016; Published: 22 March 2016

Abstract: In this paper the influence of material composition on the structural, surface and optical properties of HfO_2-TiO_2 mixed oxide coatings was investigated and discussed. Five sets of thin films were deposited using reactive magnetron sputtering: HfO_2, TiO_2 and three sets of mixed HfO_2-TiO_2 coatings with various titanium content. The change in the material composition had a significant influence on the structural, surface and optical properties. All of the deposited coatings, except for $(Hf_{0.55}Ti_{0.45})O_x$, were nanocrystalline with crystallites ranging from 6.7 nm to 10.8 nm in size. Scanning electron microscopy measurements revealed that surface of nanocrystalline thin films consisted of grains with different shapes and sizes. Based on optical transmission measurements, it was shown that thin films with higher titanium content were characterized by a higher cut-off wavelength, refractive index and lower optical band gap energy. The porosity and packing density were also determined.

Keywords: TiO_2; HfO_2; mixed oxides; optical coatings; magnetron sputtering; structural properties; optical properties

1. Introduction

Thin oxide films with precisely defined properties are a strong requirement for the development of modern technologies. Transparent thin films based on titanium dioxide (TiO_2) and hafnium dioxide (HfO_2) are widely used in industrial applications such as optical and protective coatings or optoelectronic devices. HfO_2 and TiO_2 are characterized by many advantages, e.g., very good thermal, chemical, and mechanical stability and high transparency [1–5]. Both are also known as hard oxides with high wear and scratch resistance to mechanical damage.

Due to a high transmittance over a wide spectral range from the ultraviolet (200 nm) to near-infrared (1.2 μm), low optical absorption and dispersion [6–8], high reactive index (about 1.85–2.15) [2,9], wide band gap energy (E_g = 5.8 eV) [1,10] and hydrophobic properties [2,9], hafnium dioxide is one of the most commonly used materials in optical applications [11,12]. Depending on the conditions, hafnium oxide can exist in one of the three polymorphous forms. Monoclinic crystal structure is the most thermodynamically stable form at ambient temperature and pressure; however, in temperatures above 1700 °C it transforms into a tetragonal structure, and into a cubic one above 2200 °C [3,4,6,13,14]. Thin films based on HfO_2 are frequently used as innovative materials in numerous optical devices such as optical filters, ultraviolet heat mirrors, antireflection coatings and in cameras used for space applications [2,15]. According to the literature [11,12], amorphous HfO_2 films

can be also used in flexible thin film capacitors, fiber-optic waveguides, computer memory elements and optical coatings deposited on polymer substrates.

The physical properties of titanium dioxide are also very good compared to HfO_2. Titanium dioxide is one of the basic "high index" materials, which can be used in the construction of optical coatings, for example [16]. Due to its high refractive index (2.2–2.6), high dielectric constant, optical transmittance in the visible range and photocatalytic activity, TiO_2 is used in various fields of industry [1]. TiO_2 thin films can be used in antireflective and protective coatings, self-cleaning and gas sensing films. It is also applied in solar cells and as antibacterial coatings [17–19]. This metal oxide can exist in one of the three crystal structures: anatase (E_g = 3.2–3.3 eV), rutile (E_g = 3.0–3.1 eV) or rarely applied brookite [20]. One can also distinguish mixtures of anatase and rutile or amorphous form. Anatase is metastable and transforms into the rutile at high temperature (*ca.* 700 °C) [17–22]. Rutile is the most stable phase of TiO_2. Titanium dioxide thin films with a rutile phase exhibit high refractive index and good thermal stability [21,22]. According to Lin *et al.* [21], TiO_2 thin films with a dominant rutile phase showed much greater hardness and Young's modulus values than the anatase thin films. On the other hand, an anatase phase has higher photocatalytic activity [20,21].

Hafnium and titanium thin films can be prepared using various deposition methods, for example, the sol-gel method, electron beam evaporation, ion beam assisted deposition, chemical vapor deposition, direct current (DC) or radio frequency (RF) magnetron sputtering, atomic layer deposition, *etc.* [5,9,14,15,19–21].

In the literature, the HfO_2-TiO_2 pseudobinary systems have been investigated previously by others [17,23–25], especially in view of their electrical properties [26–28]. As was shown by Li *et al.* [26], mixed oxides of HfO_2-TiO_2 had, for example, higher permittivity compared to undoped HfO_2. In the case studies performed by Triyoso *et al.*, the results revealed that mixed HfO_2-TiO_2 oxide and nanolaminate structures had improved charge trapping behavior as compared to undoped HfO_2 or TiO_2. On the other hand, Deen *et al.* [27] showed results that demonstrated enhanced electrical properties of high-k gate dielectrics based on a HfO_2/TiO_2 multilayer stack. Sequentially deposited HfO_2/TiO_2 thin layers lead to minimizing the gate oxide's physical thickness, while the gate leakage current suppression characteristics for the 2 + 5 nm thick films were shown to be equivalent to the 10 nm thick TiO_2 films [28]. Therefore, such mixtures can combine the advantages of HfO_2 and TiO_2. These thin films can also exhibit high hardness and very good optical parameters, e.g., a low extinction coefficient [1]. Due to these qualities, mixed HfO_2-TiO_2 thin films can be used as functional optical coatings.

In this paper, the influence of composition of mixed hafnium-titanium thin films deposited by reactive magnetron sputtering on their structural, surface and optical properties have been described.

2. Experimental Section

Magnetron sputtering is one of the most efficient industrial methods for manufacturing thin-film optical coatings. Manufacturing of mixed oxide thin films usually requires sputtering of alloy or powder targets with defined chemical composition. In this work, HfO_2-TiO_2 mixed oxide coatings were prepared with the aid of a multitarget magnetron sputtering apparatus as a result of the simultaneous co-sputtering of Hf (99.5%) and Ti (99.99%) targets mounted on individually supplied magnetrons [29–31]. Applied system allows for the deposition of composite coatings from up to four targets. The distribution of the power supplied to each magnetron and their sputtering time were precisely controlled, which was possible due to application of a special control system that is managing the work of MSS2 (DORA Power System) power supply units. The power released to each magnetron is controlled by the *pulse width modulation* method. The distance between the targets and substrates was equal to 160 mm. The base pressure in the deposition chamber was *ca.* 5×10^{-5} mbar, while during the sputtering process it was equal to 2×10^{-2} mbar. Thin films were sputtered in pure oxygen, without argon as a working gas. Five sets of thin films were prepared: HfO_2, TiO_2 and three HfO_2-TiO_2 mixed oxides with various material composition. The thin films were deposited on several silicon and fused

silica substrates with a size of 20 × 20 mm^2. The silicon substrates were used to assess the material composition of deposited coatings, while the glass substrates were to determine the structural and optical properties. Substrates were not heated during the deposition processes.

The surface morphology of the thin films and their chemical composition were investigated using a FESEM FEI Nova NanoSEM 230 scanning electron microscope equipped with an EDS spectrometer (EDAX Genesis, EDAX Inc., Mahwah, NJ, USA). EDS measurements were performed five times for samples from each deposition process. The EDS used for measurements was calibrated for quantitative analysis and was accurate for qualitative analysis from approximately 0.1 at.%, while for quantitative analysis from *ca.* 1 at.% of the element content. The differences in material composition of the samples from various sputtering processes were negligible and beyond the error of measurement apparatus. Additionally, SEM images of the surface of deposited thin films were obtained.

The structural properties of TiO_2, HfO_2 and their mixtures were determined based on the results of X-ray diffraction (XRD). For the measurements, a PANalytical Empyrean PIXel3D powder diffractometer with Cu Kα X-ray (1.5406 Å) was used. The correction for the broadening of the XRD instrument was accounted for and the crystallite sizes were calculated using Scherrer's equation [32].

Optical properties were evaluated on the basis of the transmission measurements. The experimental system was based on an Ocean Optics QE 65000 spectrophotometer and a coupled deuterium-halogen light source. Each transmission spectrum was averaged from five measurements performed for sample with various material compositions. Based on the obtained results, the cut-off wavelength, fundamental absorption edge and optical band gap energy (E_g) were determined. Changes of the cut-off wavelength were very small and in each case equal to *ca.* 2 nm, which was a value of inaccuracy of the measurement apparatus. A standard deviation of optical band gap energy was also calculated. Additionally, with the aid of reverse engineering method and SCOUT software, the refractive index (n) and extinction coefficient (k) were estimated.

3. Results and Discussion

The X-ray microanalysis was performed to investigate the titanium content in the deposited mixed HfO_2-TiO_2 coatings and revealed that it was equal to 17, 28 and 45 at.%, without taking into consideration signals from oxygen. In Figure 1, an exemplary distribution map of Hf, Ti and O elements in $(Hf_{0.83}Ti_{0.17})O_x$ thin film is shown, and it could be concluded that each element was homogenously distributed in the prepared coating. The area of investigation was *ca.* 16 µm × 12 µm. The EDS spectra, which show lines from Ti and Hf elements for each thin film, are also presented in Figure 1.

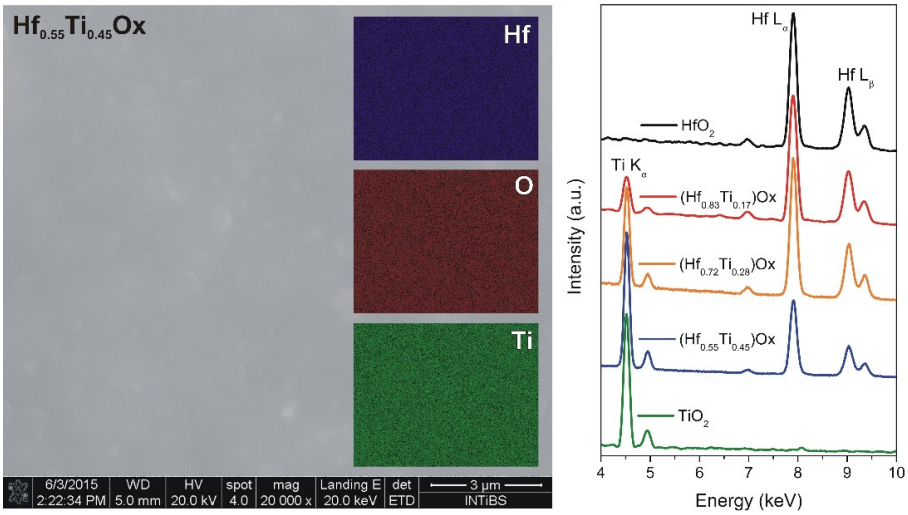

Figure 1. Secondary electron image showing Hf, Ti and O elements distribution in the $(Hf_{0.55}Ti_{0.45})O_x$ thin film and EDS spectra of as-deposited HfO_2, mixed HfO_2-TiO_2 and TiO_2 thin films

The XRD patterns for as-deposited HfO_2, mixed HfO_2-TiO_2 and TiO_2 thin films are shown in Figure 2. The hafnium dioxide, due to strong and wide diffraction lines, exhibited the nanocrystalline structure of a monoclinic phase with an average crystallites size of *ca.* 10.7 nm. Thin films with 17 and 28 at.% of titanium exhibited smaller crystallites, of 6.7 and 7.4 nm, respectively. However, further increase of the titanium concentration to 45 at.% in the prepared thin films resulted in a broad, amorphous-like pattern without visible peaks, which could be associated with hafnium dioxide or titanium dioxide phases. Therefore, it can be assumed that such increase of the titanium concentration hinders the crystal growth of prepared mixed oxide thin films. The amorphization of this coating might be caused by the introduction of the local lattice imperfections or very large mismatch of the HfO_2 and TiO_2 unit cell volume. For hafnium its unit cell volume is equal to ca. 140.3 $Å^3$, while for titanium it is only ca. 62.4 $Å^3$. This, in turn, can lead to the strong growth of the amorphous phase, which began to predominate over the crystalline structure. Similar behavior has been already observed for even small addition of *ca.* 10 at.% of Nd_2O_3 to TiO_2 thin films [33]. In the case of TiO_2, XRD measurements revealed a trace amount of fine crystallites related to the rutile phase. However, the peak at *ca.* 27.4 degrees (2θ) corresponding to the (110) rutile plane was broad and had very low intensity. Therefore, determined crystallites size of *ca.* 10.6 nm might be encumbered with small error. The broadening and low intensity of this peak can also indicate the appearance of a large amount of amorphous phase.

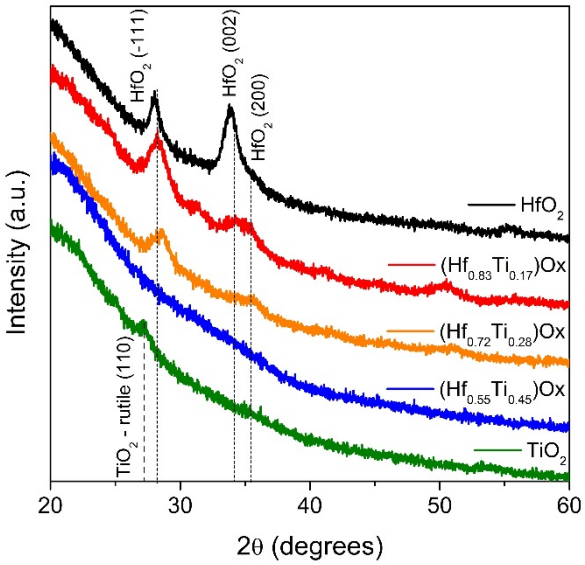

Figure 2. X-ray diffraction (XRD) measurements results of HfO_2, mixed HfO_2-TiO_2 and TiO_2 thin films.

In the case of HfO_2 thin film, XRD measurements revealed a considerable shift of the diffraction peaks towards lower angle (2θ), which indicates presence of tensile stress. The addition of 17 and 28 at.% of titanium resulted in a shift towards a higher angle. However, tensile stress still occurred in the thin film that contain 17 at.% of Ti, while for a coating with 28 at.% of Ti, compressed stress was observed. For TiO_2, tensile stress was again observed. The type of stress occurring in measured coatings was determined on the basis of the Δd parameter from the following equation [34]:

$$\Delta d = \frac{d - d_{PDF}}{d_{PDF}} \times 100\% \quad (1)$$

where d—interplanar distance, d_{PDF}—the standard interplanar distance from [35,36].

Results of XRD measurements and analysis are presented in Table 1. The positive sign of the Δd parameter speaks to tensile stress and the negative to the compressed one.

SEM images of the surface of as-deposited thin films are shown in Figure 3. All sputtered coatings were crack-free and continuous. HfO_2 thin films consisted of small grains with dimensions of *ca.*

20–30 nm. In the case of $(Hf_{0.83}Ti_{0.17}O)_x$ thin film its surface was built from grains with round shapes, which had various dimensions in the range from *ca.* 25 nm to 95 nm. For $(Hf_{0.72}Ti_{0.28})O_x$, the coating of its surface consisted of grains with round shapes of mostly small sizes of *ca.* 15–25 nm, however also few grains with larger size of *ca.* 50 nm were visible. A larger amount of Ti in the film, *i.e.*, 45 at.%, resulted in a significant change to the surface morphology. The surface of this thin film was homogenous, very smooth and no grains were observed. SEM image confirmed the XRD results, which showed amorphous behavior of the investigated coating. In the case of the TiO_2 thin film, its surface was covered with particles of different shapes with various dimensions in the range from 30 nm to as much as 150 nm.

Table 1. XRD measurements results for as-deposited HfO_2, mixed HfO_2-TiO_2 and TiO_2 thin films.

Thin Film	Crystal Plane	D (nm)	*d* (Å)	Δ*d* (%)	Type of Stress
PDF No. 65-1142 HfO_2–monoclinic [35]	(−111)	–	3.145	–	–
PDF No. 21-1276 TiO_2–rutile [36]	(110)	–	3.247	–	–
HfO_2	(−111)	10.7	3.171	+0.81	tension
$(Hf_{0.83}Ti_{0.17})O_x$		6.7	3.155	+0.32	tension
$(Hf_{0.72}Ti_{0.28})O_x$		7.4	3.129	−0.53	compression
$(Hf_{0.55}Ti_{0.45})O_x$	amorphous	–	–	–	–
TiO_2	(110)	10.8	3.261	+0.43	tension

D—average crystallite size; *d*—interplanar distance; Δ*d*—percentage change of interplanar distance as-compared to standard (d_{PDF}) one.

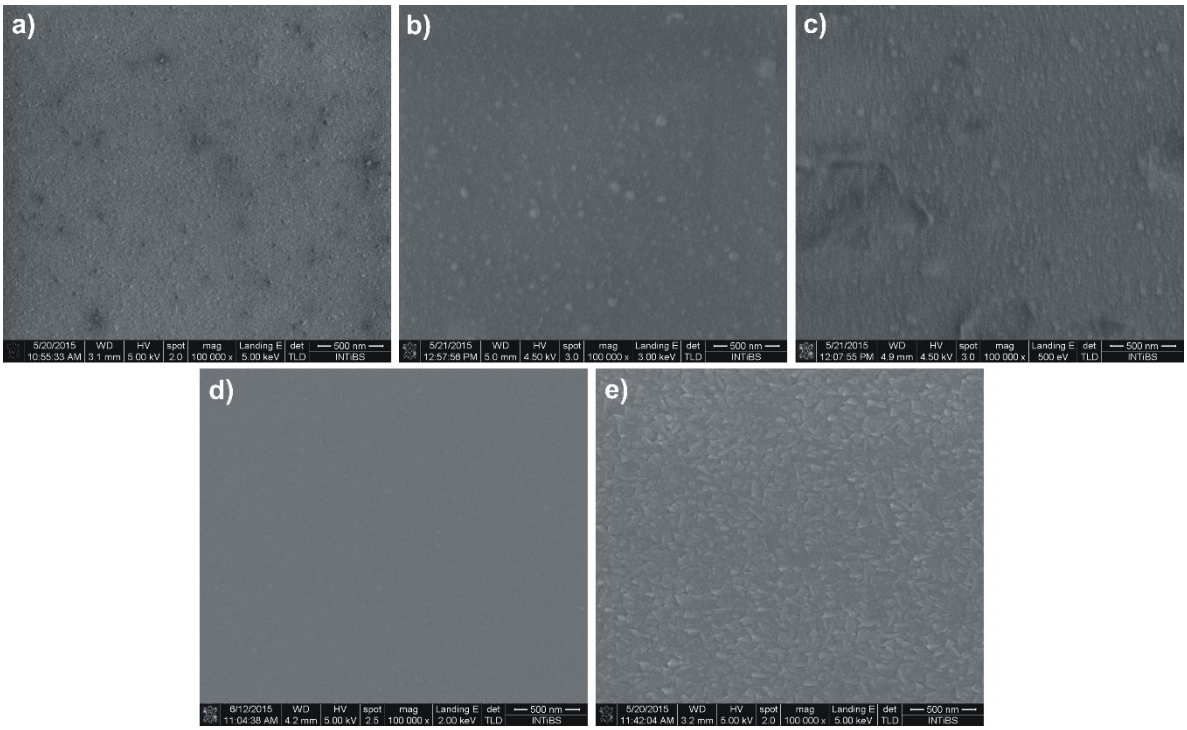

Figure 3. SEM images of the surface of: (**a**) HfO_2; (**b**) $(Hf_{0.83}Ti_{0.17})O_x$; (**c**) $(Hf_{0.72}Ti_{0.28})O_x$; (**d**) $(Hf_{0.55}Ti_{0.45})O_x$; (**e**) TiO_2 thin films.

Optical properties such as cut-off wavelength ($\lambda_{cut\text{-}off}$) and optical band gap energy (E_g) were determined based on transmission spectra measurements in the range from *ca.* 200 nm to 1000 nm. The results of these measurements and analysis are presented in Figure 4. All as-deposited thin

films were transparent in the visible wavelength range with the transmittance level of approximately 80%–90%, depending on the content of titanium. The highest average transmission was exhibited by pure hafnium, while the lowest (with the largest amplitude of optical interferences) was obtained for undoped titanium.

The results of cut-off wavelength measurements for all thin films are compared in Figure 4b. For hafnium, it is lower than 200 nm within the measured spectral range. The addition of 17 at.% of titanium to the thin film resulted in a significant shift of $\lambda_{cut\text{-}off}$ towards longer wavelength, *i.e.*, 277 nm. Further increases in titanium content to 28 at.% and 45 at.% caused a shift in $\lambda_{cut\text{-}off}$ to 298 nm and 310 nm, respectively. In the case of undoped titanium, $\lambda_{cut\text{-}off}$ is equal to 344 nm. It seems that increasing the titanium content to HfO_2 caused a redshift of the cut-off wavelength. The estimation of the absorption edge (Figure 4c) showed that it has decreased with the increase of titanium content in the thin film from 6.84 eV for undoped HfO_2 to 3.27 eV for pure TiO_2.

The optical band gap energy is shown in Figure 4c and was determined from Tauc plots $(\alpha h\nu)^{1/2}$ in the function of photon energy (eV). It is important to estimate the optical band gap energy since it shows the energy needed for the transfer of the electron from the valence to the conduction band. For pure hafnium, E_g is equal to 6.08 eV for indirect transitions. The addition of 17 at.% of titanium caused a decrease in the value of the optical band gap to 3.41 eV. Further increases of the titanium amounts in deposited thin films to 28 at.% and 45 at.% caused a small, but gradual decrease of the optical band to 3.39 eV and 3.36 eV. The lowest value of E_g was obtained for undoped TiO_2, equal to 3.11 eV. Similarly to the cut-off wavelength, the change of the value of optical band gap is caused by the increase of TiO_2 content in the mixed oxide thin films.

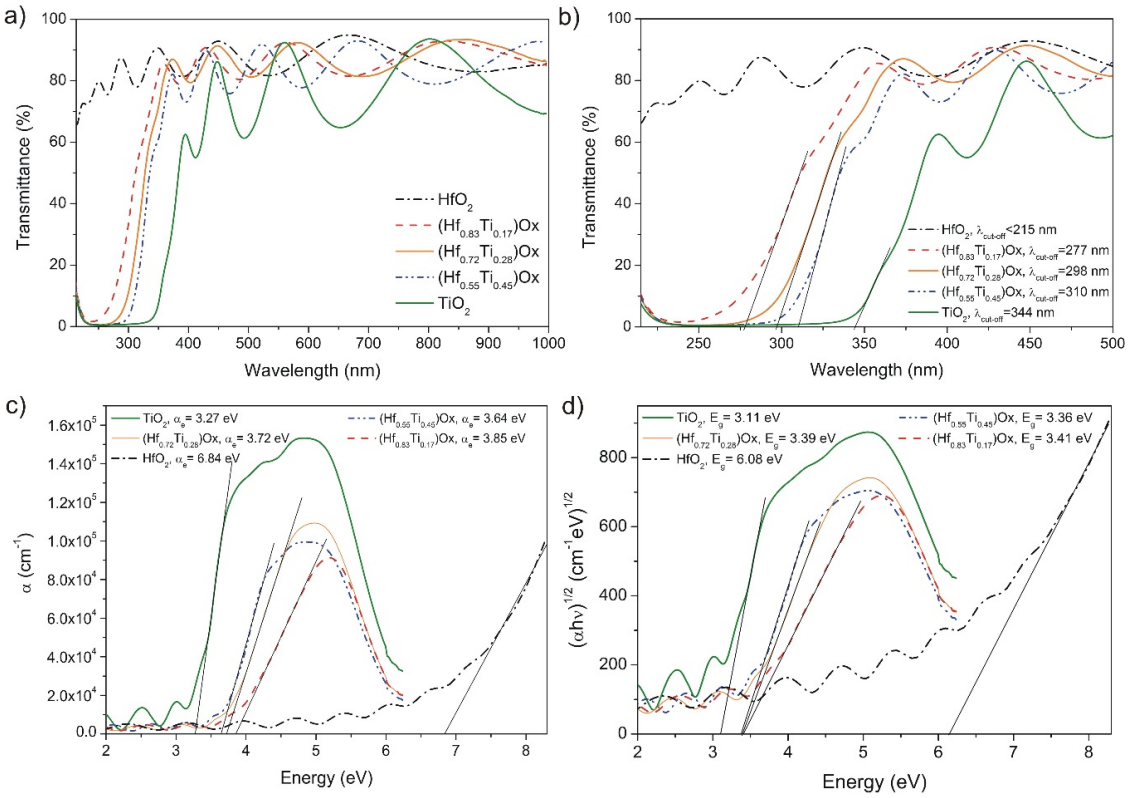

Figure 4. Results of optical investigations of as-deposited thin films: (**a**) transmittance spectra; (**b**) transmittance spectra with magnified area for the purpose of cut-off wavelength ($\lambda_{cut\text{-}off}$) determination; (**c**) absorption edge; (**d**) optical band gap energy.

In Figure 5, the spectral characteristics of the refractive index (n) and extinction coefficient (k) are presented. For the calculation of n and k dispersion curves, the reverse engineering method was

used with the aid of SCOUT software [37]. Additionally, the thickness of each of the samples was also estimated. TiO_2 and HfO_2 thin films were sputtered from single Ti or Hf metallic targets. Their thickness was similar and equal to 359 nm and 371 nm, respectively. Thin films of mixed HfO_2-TiO_2 coatings were sputtered from two independently powered targets, and the thickness of $Hf_{0.83}Ti_{0.17}O_x$, $Hf_{0.72}Ti_{0.28}O_x$ and $Hf_{0.55}Ti_{0.45}O_x$ was equal to 453 nm, 472 nm and 526 nm, respectively.

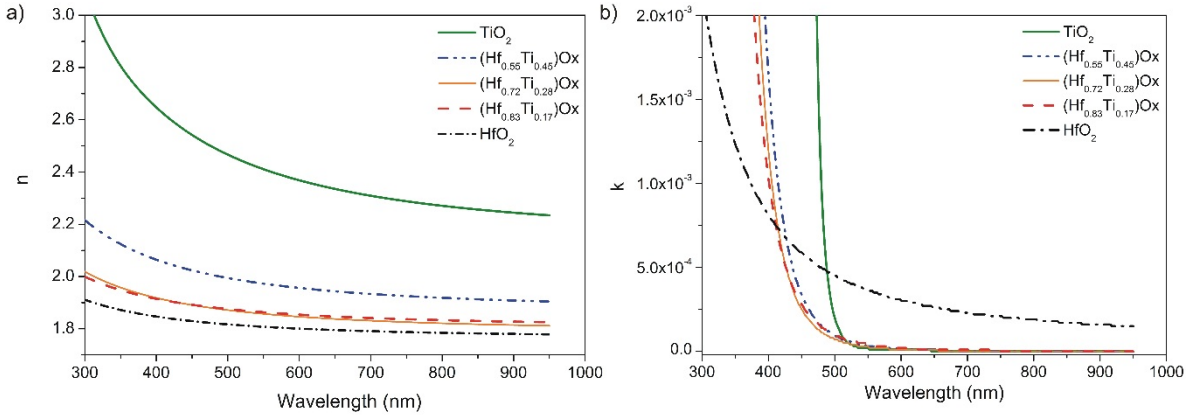

Figure 5. Optical properties of as-deposited thin films: (**a**) refractive index; (**b**) extinction coefficient.

The values of the refractive index and extinction coefficient are dependent on the TiO_2 concentration in the thin films. It was observed that with the increase of titanium content in the coatings, the refractive index gradually increased, while the extinction coefficient decreased. Changes in the refractive index and extinction coefficient determined for λ = 550 nm are presented in Figure 6a. The refractive index for as-deposited coatings increased from 1.81 for HfO_2 to 2.41 for TiO_2. The mechanism that might be related to the increase of n is directly related to the increase of the content of titanium in the thin films, which have significantly higher value than hafnium. Values of n for bulk HfO_2 with a monoclinic phase, and for TiO_2 with a rutile phase, are equal to 2.12 [38] and 2.65 [39], respectively. Therefore, the obtained values for thin films were slightly lower and stood out from the bulk ones.

Based on the obtained values of n, porosity (P) and packing density (PD) were calculated for different compositions. Porosity was estimated using following equation [40,41]:

$$P(\%) = \left[1 - \left(\frac{n_f^2 - 1}{n_b^2 - 1}\right)\right] \times 100\% \quad (2)$$

where n_f—measured refractive index of deposited thin film, n_b—refractive index of the correspondent bulk material.

In turn, the packing density (PD) of a film is defined as the ratio of the average film density (ρ_f) and the bulk density (ρ_b) according to the equation [33,40,41]:

$$PD = \frac{\rho_f}{\rho_b} \quad (3)$$

The correlation between the film refractive index and its packing density can be expressed by [40,42,43]:

$$PD = \frac{\left(n_f^2 - 1\right) \times \left(n_b^2 + 2\right)}{\left(n_f^2 + 2\right) \times \left(n_b^2 - 1\right)} \quad (4)$$

It is also necessary to determine the refractive index of the correspondent bulk material for each HfO_2-TiO_2 composition according to the Lorentz-Lorentz relationship [40,44]:

$$\frac{(n_b^2-1)}{(n_b^2+2)} = f_1 \cdot \frac{(n_1^2-1)}{(n_1^2+2)} + f_2 \cdot \frac{(n_2^2-1)}{(n_2^2+2)} \quad (5)$$

where n_1, n_2 and f_1, f_2 are the refractive indices of the bulk components and their molar ratios in the HfO_2-TiO_2 composite material, respectively.

Using a determined refractive index of deposited thin films, it can be seen that the highest porosity and simultaneously the lowest packing density was obtained for $(Hf_{0.72}Ti_{0.28})O_x$ thin films. In the case of HfO_2, $(Hf_{0.0.83}Ti_{0.17})O_x$ and $(Hf_{0.55}Ti_{0.45})O_x$ porosity was very similar. The lowest value of porosity was obtained for undoped TiO_2. Therefore, it can be assumed that titanium exhibits the most closely packed structure, which was also confirmed by the calculation of the packing density. The packing density for all HfO_2 and mixed HfO_2-TiO_2 coatings revealed only negligible changes. The results of the dependence of porosity and packing density on TiO_2 content is shown in Figure 6b. Results of optical properties measurements are summarized in Table 2.

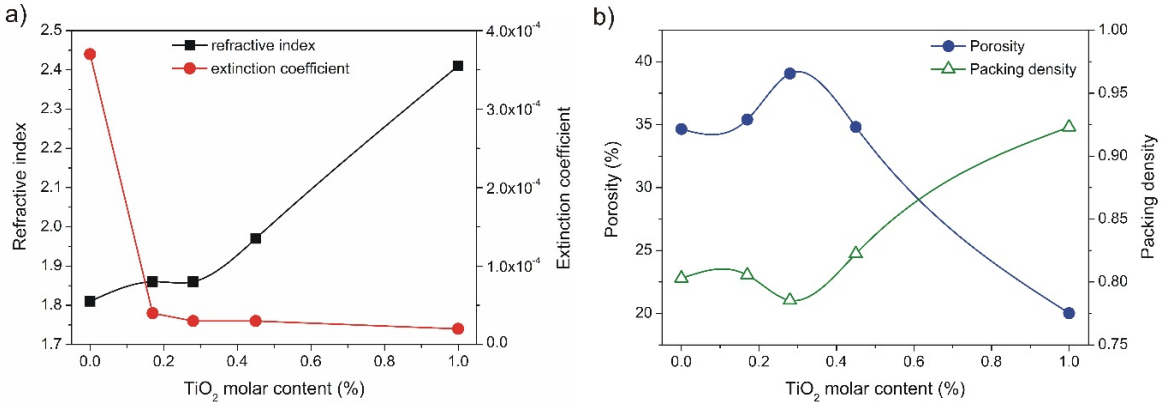

Figure 6. Dependence of: (**a**) refractive index and extinction coefficient; (**b**) porosity and packing density on TiO_2 molar content.

Table 2. Optical properties measurements result of deposited thin films

Thin Film	$\lambda_{cut\text{-}off}$ (nm)	E_g (eV)	n (at 550 nm)	k (at 550 nm)	P (%)	PD
HfO_2	<215 ± 2	6.08 ± 0.07	1.81	3.7×10^{-4}	34.7	0.80
$(Hf_{0.83}Ti_{0.17})O_x$	277 ± 2	3.41 ± 0.03	1.86	4×10^{-5}	35.4	0.81
$(Hf_{0.72}Ti_{0.28})O_x$	298 ± 2	3.39 ± 0.03	1.86	3×10^{-5}	39.1	0.79
$(Hf_{0.55}Ti_{0.45})O_x$	310 ± 2	3.36 ± 0.02	1.97	3×10^{-5}	34.8	0.82
TiO_2	344 ± 2	3.11 ± 0.02	2.41	2×10^{-5}	20.0	0.92

4. Conclusions

In this paper HfO_2, mixed HfO_2-TiO_2 and TiO_2 coatings were deposited using magnetron sputtering. Through the change in the power released by each magnetron, it was possible to obtain mixed HfO_2-TiO_2 coatings with various amount of titanium content.

The change of the titanium content in mixed oxide thin films resulted in different structural, surface and optical properties. In the case of structural properties, XRD studies revealed that except for amorphous $(Hf_{0.55}Ti_{0.45})O_x$ thin film, all of the deposited coatings were nanocrystalline. The crystallite sizes of undoped hafnium and titanium were larger than those of mixed oxides by *ca.* 50%. The increase in the amount of titanium also resulted in the change of surface morphology. SEM studies in the case

of $(Hf_{0.55}Ti_{0.45})O_x$ thin films seem to confirm the XRD measurements and speak to the amorphous behavior of this coating.

Optical properties changed significantly with the material composition of each thin film. The cut-off wavelength and refractive index increased with the increase in titanium, while the optical band gap and the extinction coefficient simultaneously decreased. It was determined that the most porous thin film, which also exhibited the lowest packing density, was $(Hf_{0.72}Ti_{0.28})O_x$. On the other hand, undoped TiO_2 had the lowest porosity and the highest packing density.

Acknowledgments: This work was financed from the sources given by the National Science Centre NCN in the years 2014-2017 as a research project No. DEC-2013/09/B/ST8/00140.

Author Contributions: Michał Mazur performed the experiments; Danuta Kaczmarek designed the experiments; Michał Mazur, Danuta Kaczmarek, Jarosław Domaradzki, Damian Wojcieszak and Agata Poniedziałek analyzed the data; Michał Mazur wrote the paper.

Conflicts of Interest: The authors declare no conflict of interest.

References

1. Mazur, M.; Wojcieszak, D.; Domaradzki, J.; Kaczmarek, D.; Poniedziałek, A.; Domanowski, P. Investigation of microstructure, micro-mechanical and optical properties of $HfTiO_4$ thin films prepared by magnetron co-sputtering. *Mater. Res. Bull.* **2015**, *72*, 116–122. [CrossRef]
2. Jain, R.K.; Gautam, Y.K.; Dave, V.; Chawla, A.K.; Chandra, R. A study on structural, optical and hydrophobic properties of oblique angle sputter deposited HfO_2 films. *Appl. Surf. Sci.* **2013**, *283*, 332–338. [CrossRef]
3. Lin, S.S.; Liao, C.S.; Fan, S.Y. Effects of substrate temperature on properties of HfO_2, HfO_2:Al and HfO_2:W films. *Surf. Coat. Technol.* **2015**, *271*, 269–275. [CrossRef]
4. Lin, S.S. Optical properties of HfO_2 nanoceramic films asa function of N-Bi co-doping. *Ceram. Int.* **2014**, *40*, 5707–5713. [CrossRef]
5. Vyas, S.; Tiwary, R.; Shubham, K.; Chakrabarti, P. Study the target effect on the structural, surface and optical properties of TiO_2 thin film fabricated by RF sputtering method. *Superlattices Microst.* **2015**, *80*, 215–221. [CrossRef]
6. Vargas, M.; Murphy, N.R.; Ramana, C.V. Structure and optical properties of nanocrystalline hafnium oxide thin films. *Opt. Mater.* **2014**, *37*, 621–628. [CrossRef]
7. Franta, D.; Ohlídal, I.; Nečas, D.; Vižd'a, F.; Caha, O.; Hasoň, M.; Pokorný, P. Optical characterization of HfO_2 thin films. *Thin Solid Films* **2011**, *519*, 6085–6091. [CrossRef]
8. Vlček, J.; Belosludtsev, A.; Rezek, J.; Houška, J.; Čapek, J.; Čerstvý, R.; Haviar, S. High-rate reactive high-power impulse magnetron sputtering of hard and optically transparent HfO_2 films. *Surf. Coat. Technol.* **2015**. [CrossRef]
9. Linn, S.S.; Li, H.R. The optical properties of hydrophilic Hf-doped HfO_2 nanoceramic films. *Ceram. Int.* **2013**, *39*, 7677–7683. [CrossRef]
10. Jena, S.; Tokas, R.B.; Misal, J.S.; Rao, K.D.; Udupa, D.V.; Thakur, S.; Sahoo, N.K. Effect of O_2/Ar gas flow ratio on the optical properties and mechanical stress of sputtered HfO_2 thin films. *Thin Solid Films* **2015**, *592*, 135–142. [CrossRef]
11. Khoshman, J.M.; Khan, A.; Kordesch, M.E. Amorphous hafnium oxide thin films for antireflection optical coatings. *Surf. Coat. Technol.* **2008**, *202*, 2500–2502. [CrossRef]
12. Khoshman, J.M.; Kordesch, M.E. Optical properties of a-HfO_2 thin films. *Surf. Coat. Technol.* **2006**, *201*, 3530–3535. [CrossRef]
13. Garcia, J.C.; Lino, A.T.; Scolfaro, L.M.R.; Leite, J.R.; Freire, V.N.; Farias, G.A.; da Silva, E.F. Band structure derived properties of HfO_2 from first principles calculations. *AIP Conf. Proc.* **2005**, *772*, 189–190.
14. Vargas, M.; Murphy, N.R.; Ramana, C.V. Tailoring the index of refraction of nanocrystalline hafnium oxide thin films. *Appl. Phys. Lett.* **2014**, *104*, 101907. [CrossRef]
15. Al-Kuhaili, M.F. Optical properties of hafnium oxide thin films and their application in energy-efficient windows. *Opt. Mater.* **2004**, *27*, 383–387. [CrossRef]
16. Mazur, M.; Morgiel, J.; Wojcieszak, D.; Kaczmarek, D.; Kalisz, M. Effect of Nd doping on structure and improvement of the properties of TiO_2 thin films. *Surf. Coat. Technol.* **2015**, *270*, 57–65. [CrossRef]

17. Domaradzki, J.; Kaczmarek, D.; Prociow, E.L.; Borkowska, A.; Kudrawiec, R.; Misiewicz, J.; Schmeisser, D.; Beuckert, G. Characterization of nanocrystalline TiO_2-HfO_2 thin films prepared by low pressure hot target reactive magnetron sputtering. *Surf. Coat. Technol.* **2006**, *200*, 6283–6287. [CrossRef]
18. Twu, M.J.; Chiou, A.H.; Hu, C.C.; Hsu, C.Y.; Kuo, C.G. Properties of TiO_2 films deposited on flexible substrates using direct current magnetron sputtering and using high power impulse magnetron sputtering. *Polym. Degrad. Stabil.* **2015**, *117*, 1–7. [CrossRef]
19. Choi, K.H.; Duraisamy, N.; Muhammad, N.M.; Kim, I.; Choi, H.; Jo, J. Structural and optical properties of electrohydrodynamically atomized TiO_2 nanostructured thin films. *Appl. Phys. A* **2012**, *107*, 715–722. [CrossRef]
20. Bedikyan, L.; Zakhariev, S.; Zakharieva, M. Titanium dioxide thin films: preparation and optical properties. *J. Chem. Tech. Metall.* **2013**, *48*, 555–558.
21. Lin, J.; Wang, B.; Sproul, W.D.; Ou1, Y.; Dahan, I. Anatase and rutile TiO_2 films deposited by arc-free deep oscillation magnetron sputtering. *J. Phys. D Appl. Phys.* **2013**, *46*, 084008. [CrossRef]
22. Heo, C.H.; Lee, S.B.; Boo, J.H. Deposition of TiO_2 thin films using RF magnetron sputtering method and study of their surface characteristics. *Thin Solid Films* **2005**, *475*, 183–188. [CrossRef]
23. Cisneros-Morales, M.C.; Aita, C.R. Crystallization, metastable phases, and demixing in a hafnia-titania nanolaminate annealed at high temperature. *J. Vac. Sci. Technol. A* **2010**, *28*, 1161–1168. [CrossRef]
24. Chen, F.; Bin, X.; Hella, C.; Shi, X.; Gladfelter, W.L.; Campbell, S.A. A study of mixtures of HfO_2 and TiO_2 as high-k gate dielectrics. *Microelectron. Eng.* **2004**, *72*, 263–266. [CrossRef]
25. Zhang, J.W.; Hea, G.; Zhou, L.; Chen, H.S.; Chen, X.S.; Chen, X.F.; Deng, B.; Lv, J.G.; Sun, Z.Q. Microstructure optimization and optical and interfacial properties modulation of sputtering-derived HfO_2 thin films by TiO_2 incorporation. *J. Alloy. Compd.* **2014**, *611*, 253–259. [CrossRef]
26. Li, H.J.; Price, J.; Gardner, M.; Lu, D.; Kwong, D.L. High permittivity quaternary metal ($HfTaTiO_x$) oxide layer as an alternative high-k gate dielectric. *Appl. Phys. Lett.* **2006**, *89*, 103523. [CrossRef]
27. Deen, D.A.; Champlain, J.G.; Koester, S.J. Multilayer HfO_2/TiO_2 gate dielectric engineering of graphene field effect transistors. *Appl. Phys. Lett.* **2013**, *103*, 073504. [CrossRef]
28. Triyoso, D.H.; Hegde, R.I.; Wang, X.D.; Stoker, M.W.; Rai, R.; Ramon, M.E.; White, B.E., Jr.; Tobin, P.J. Characteristics of mixed oxides and nanolaminates of atomic layer deposited HfO_2-TiO_2 gate dielectrics. *J. Electrochem. Soc.* **2006**, *153*, 834–839. [CrossRef]
29. Kaczmarek, D.; Domaradzki, J.; Adamiak, B.; Dora, J.; Maguda, S. A Method of Depositing Films in the Multitarget System for Magnetron Sputtering. Pol. Pat. Appl. PL396389, 2011.
30. Mazur, M.; Kalisz, M.; Wojcieszak, D.; Grobelny, M.; Mazur, P.; Kaczmarek, D.; Domaradzki, J. Determination of structural, mechanical and corrosion properties of Nb_2O_5 and $(Nb_yCu_{y-1})O_x$ thin films deposited on Ti_6Al_4V alloy substrates for dental implant applications. *Mater. Sci. Eng.* **2015**, *47*, 211–221. [CrossRef] [PubMed]
31. Kalisz, M.; Grobelny, M.; Mazur, M.; Wojcieszak, D.; Świniarski, M.; Zdrojek, M.; Domaradzki, J.; Kaczmarek, D. Mechanical and electrochemical properties of Nb_2O_5, Nb_2O_5:Cu and graphene layers deposited on titanium alloy (Ti_6Al_4V). *Surf. Coat. Technol.* **2015**, *271*, 92–99. [CrossRef]
32. Klug, H.P.; Alexander, L.E. *X-ray Diffraction Procedures for Polycrystalline and Amorphous Materials*, 2nd ed.; John Wiley and Sons: New York, NY, USA, 1974.
33. Mazur, M.; Howind, T.; Gibson, D.; Kaczmarek, D.; Song, S.; Wojcieszak, D.; Wenzhong, Z.; Mazur, P.; Domaradzki, J.; Placido, F. Investigation of structural, optical and micro-mechanical properties of $(Nd_yTi_{1-y})O_x$ thin films deposited by magnetron sputtering. *Mater. Design* **2015**, *85*, 377–388. [CrossRef]
34. Domaradzki, J.; Kaczmarek, D.; Prociow, E.; Wojcieszak, D.; Sieradzka, K.; Mazur, M.; Lapinski, M. Study of structural and optical properties of TiO_2:Tb thin films prepared by high energy reactive magnetron sputtering method. *Opt. Appl.* **2009**, *39*, 815–823.
35. Powder Diffraction File, Card 34–0104, Joint Committee on Powder Diffraction Standards, Philadelphia, PA, USA, 1984.
36. Powder Diffraction File, Card 21–1276, Joint Committee on Powder Diffraction Standards, Philadelphia, PA, USA, 1967.
37. W.Theiss Hard- and Software. Available online: http://www.mtheiss.com (accessed on 18 March 2016).
38. Wood, D.L.; Nassau, K.; Kometani, T.Y.; Nash, D.L. Optical properties of cubic hafnium stabilized with yttria. *Appl. Opt.* **1990**, *29*, 604–607. [CrossRef] [PubMed]

39. Devore, J.R. Refractive Indices of Rutile and Sphalerite. *J. Opt. Soc. Am.* **1951**, *41*, 416–419. [CrossRef]
40. Kermadi, S.; Agoudjil, N.; Sali, S.; Zougar, L.; Boumaour, M.; Broch, L.; Naciri, A.En.; Placido, F. Microstructure and optical dispersion characterization of nanocomposite sol-gel TiO_2-SiO_2 thin films with different compositions. *Spectrochim. Acta A* **2015**, *145*, 145–154. [CrossRef] [PubMed]
41. Subramanian, M.; Vijayalakshmi, S.; Venkataraj, S.; Jayavel, R. Effect of cobalt doping on the structural and optical properties of TiO_2 films prepared by sol-gel process. *Thin Solid Films* **2008**, *516*, 3776–3782. [CrossRef]
42. Dave, V.; Dubey, P.; Gupta, H.O.; Chandra, R. Influence of sputtering pressure on the structural, optical and hydrophobic properties of sputtered deposited HfO_2 coatings. *Thin Solid Films* **2013**, *549*, 2–7. [CrossRef]
43. Bauer, G. Absolutwerte der optischen Absorptionskonstanten von Alkalihalogenidkristallen im Gebiet ihrer ultravioletten Eigenfrequenzen. *Ann. Phys.* **1934**, *411*, 434–464. [CrossRef]
44. Humard, M.; Riassetto, D.; Roussel, F.; Bourgeois, A.; Berthome, G.; Joud, J.C.; Langlet, M. Enhanced persistence of natural super-hydrophilicity in TiO_2-SiO_2 composite thin films deposited via a sol-gel route. *Surf. Sci.* **2008**, *602*, 3364–3374. [CrossRef]